Myosin mRNA Accumulation and Myofibrillogenesis at the Myotendinous Junction of Stretched Muscle Fibers

David J. Dix and Brenda R. Eisenberg

Department of Physiology and Biophysics, University of Illinois School of Medicine, Chicago, Illinois 60612

Abstract. Myofiber growth and myofibril assembly at the myotendinous junction (MTJ) of stretch-hypertrophied rabbit skeletal muscle was studied by in situ hybridization, immunofluorescence, and electron microscopy. In situ hybridization identified higher levels of myosin heavy chain (MHC) mRNA at the MTJ of fibers stretched for 4 d. Electron microscopy at the MTJ of these lengthening fibers revealed a large cytoplasmic space devoid of myofibrils, but containing polysomes, sarcoplasmic reticulum and T-membranes, mitochondria, Golgi complexes, and nascent filament assemblies. Tallies from electron micrographs indicate that myofibril assembly in stretched fibers followed a set sequence of events. (*a*) In stretched fiber ends almost the entire sarcolemmal membrane was electron dense but only a portion had attached myofibrils. Vinculin, detected by immunofluorescence, was greatly increased at the MTJ membrane of stretched muscles. (*b*) Thin filaments were anchored to the sarcolemma at the electron dense sites. (*c*) Thick filaments associated with these thin filaments in an unregistered manner. (*d*) Z-bodies splice into thin filaments and subsequently thin and thick filaments fall into sarcomeric register. Thus, the MTJ is a site of mRNA accumulation which sets up regional protein synthesis and myofibril assembly. Stretched muscles also lengthen by the addition of myotubes at their ends. After 6 d of stretch these myotubes make up the majority of fibers at the muscle ends. Essentially all these myotubes repeat the developmental program of primary myotubes and express slow MHC. MHC mRNA distribution in myotubes is disorganized as is the distribution of their myofibrils.

FIBER lengthening in response to stretch creates a need for rapid contractile protein synthesis and assembly into myofibrils at the myotendinous junction (MTJ).[1] It was first suggested that muscle fibers lengthen by adding sarcomeres at the MTJ in 1927 (Schmidt, 1927). During stretch-induced growth sarcomeres are added in series at fiber ends (Williams and Goldspink, 1973; Goldspink, 1985) making this model of rapid growth ideal for the study of myofibrillogenesis and mRNA localization.

Several examples of the subcellular distribution of mRNA matching the distribution of the protein encoded have been reported in muscle cells and tissue. Acetylcholine receptor mRNA and protein accumulates at the neuromuscular junctions of skeletal fibers (Fontaine et al., 1988; Merlie and Sanes, 1985). In cultured myoblasts and fibroblasts actin, vimentin and tubulin mRNAs concentrate in regions where their respective proteins assemble (Lawrence and Singer, 1986). In normal muscle fibers, myosin heavy chain (MHC) mRNA is most concentrated around the nuclei under the sarcolemmae (Dix and Eisenberg, 1988). Local synthesis of MHC may be required due to the competing forces of MHC diffusion versus assembly. Rapid self-assembly of MHC and exchange with existing thick filaments and sarcomeres could limit the rate of protein diffusion (Bouche et al., 1988; Johnson et al., 1988; Saad et al., 1986; Wenderoth and Eisenberg, 1987). The large size of the MHC molecule also slows diffusion in the highly structured myofibril lattice (Eisenberg et al., 1989).

There are at least three current models of myofibril assembly, none of which is inherently exclusive of the others. One model theorizes that association of myosin into thick filaments is mediated by actin filament networks (Mahajan et al., 1989). Evidence suggests that myosin molecules first bind to actin filaments, then translocation along the length of the actin filament increases the probability of myosin–myosin interactions and the formation of thick filaments. A second model identifies stress fiber–like structures as the primary template for forming myofibrils (Antin et al., 1986; Dlugosz et al., 1984). Stress fiber–like structures are actin filament bundles that form in many cell types including under the sarcolemmae of cultured cardiac cells. A third model calls attention to the importance of Z-band formation (α-actinin) for thick filament addition to myofibrils (Sanger et

This is a partial requirement for the Ph.D. thesis for D. J. Dix.

D. J. Dix's present address is Department of Biochemistry, North Carolina State University, Raleigh, NC 27695-7622.

1. *Abbreviations used in this paper*: MHC, myosin heavy chain; MTJ, myotendinous junction; TA, tibialis anterior.

al., 1986). They propose the formation of closely spaced, linear arrays of Z-bodies into minisarcomeres at an early stage of myofibrillogenesis. A variation of this third model has titin filaments organized about the Z-bodies, setting a register through the I-bands on either side of the Z-bodies while myosin filaments organize into the A-band (Hill et al., 1986; Lin et al., 1989; Tokuyasu and Maher, 1987*a*, *b*). It is possible that invertebrate muscle follows a different assembly pattern but it is of interest to note that in mutant *Drosophila* I-Z-I segments can assemble without A-bands and conversely A-bands can form without I-Z-I segments (Beall et al., 1989; O'Donnell and Bernstein, 1988). The MTJ of stretched fibers are rich in examples to compare with all these models of myofibrillogenesis.

Elongating fibers of stretched muscles have large accumulations of mRNA and polysomes at their MTJ. These stretched fibers also exhibit structural changes related to sarcomere assembly and myofibril-membrane attachment at the growing tip. Mechanisms directing regional growth and assembly in these stretched fibers are discussed with regard to these observations.

Materials and Methods

Animals and Tissue

Governmental and institutional guidelines for animal care and use were followed at all times. A total of eight female New Zealand White rabbits (~2.5 kg body weight) provided tibialis anterior (TA) muscles. Stretching of the TA was accomplished by casting the lower hindlimb in full plantar flexion for either 4 or 6 d. Soft casts made up of tongue depressors and cloth tape were applied to rabbits anesthetized with an intramuscular injection of Acepromazine maleate and Ketamine HCl (0.8 and 35 mg, respectively, per kilogram body weight). The muscles were removed from the stretched and contralateral control muscle, blotted dry, weighed, and the lengths measured. Blocks of tissue for in situ hybridization (ISH) and immunofluorescence were flash frozen in isopentane cooled with liquid nitrogen and then stored at −80°C in isopentane until use. Blocks of tissue for electron microscopy were fixed in 2.5% glutaraldehyde in 0.1 M cacodylate, stained with lead citrate and uranyl acetate, and embedded in plastic resin.

In Situ Hybridization

Hybridizations were performed as previously described (Dix and Eisenberg, 1988). RNA probes were transcribed from the 1,107-bp rabbit α-cardiac MHC cDNA pBMHC-1 (Sinha et al., 1984). Biotin-11-UTP (Bethesda Research Laboratories, Gaithersburg, MD) substituted for UTP in transcription reactions for both RNA strands, the sense strand probe was used to control for nonspecific background binding levels. Frozen sections (8–10 μm) were fixed with 4% paraformaldehyde in PBS, 5 mM $MgCl_2$ for 15 min. Sections were usually cut and fixed the same day they were to be hybridized, or were stored fresh frozen at −20°C overnight.

After hybridization with the biotinylated probes, the sections were incubated on 20 ng/μl ribonuclease A and washed extensively to remove unhybridized probe. Enzymatic detection of the biotin label was done with streptavidin-alkaline phosphatase (SAP; Clontech Laboratories, Inc., Palo Alto, CA). Sections were viewed and photographed with a Nikon Microphot-FXA.

Immunofluorescence

Immunofluorescent detection of slow MHC protein was accomplished on frozen sections with the monoclonal antibody HPM-7 at 1:2,000 dilution (Kennedy et al., 1986; a kind gift of Dr. R. Zak, University of Chicago). Slow specificity of HPM-7 in rabbit was confirmed by comparison with ATPase-stained serial sections. Monoclonal antibody to vinculin (Sigma Chemical Co., St. Louis, MO) was used at 1:50 dilution.

Unfixed frozen sections were pretreated with newborn calf serum and incubated with the primary antibody. Sections were rinsed and then treated with the appropriate secondary antibody. Sections were viewed and photographed with a Nikon Microphot-FXA with indirect immunofluorescence.

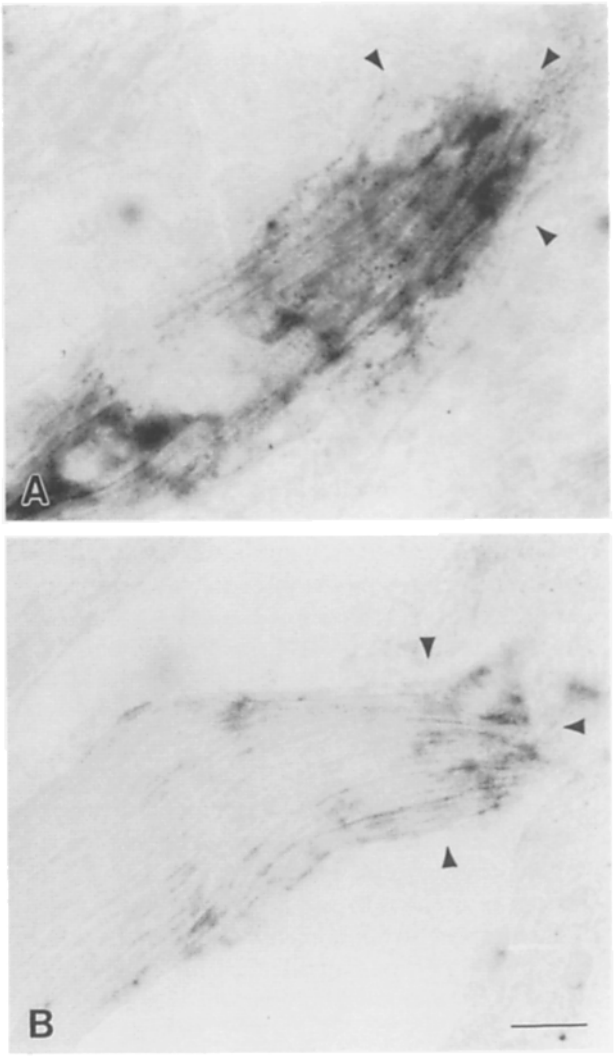

Figure 1. In situ hybridization of slow MHC mRNA at the MTJ of slow-oxidative fibers from 4-d stretched and control TA. The region was identified as being the termination of the fiber by phase microscopy (not shown). (*A*) Stretched fiber with dense, unordered accumulation of mRNA at its MTJ (*arrowheads*). (*B*) Control fiber with less accumulation of mRNA at the MTJ (*arrowheads*). Bar, 10 μm.

Electron Microscopy

Sections from stretched and control TA were stained and observed with a JEOL 100 CX electron microscope. Survey electron micrographs of both transverse and longitudinal sections were taken at 7,500–30,000-fold final magnification.

Membrane content at the myotendinous junction of fibers was determined using published methods (Eisenberg and Milton, 1984). 6 control fibers from 2 muscles and 15 stretched fibers from 4 muscles were randomly selected. Total fiber areas sampled for control (1,270 μm^2 in 20 micrographs) and stretched fibers (10, 166 μm^2 in 60 micrographs) were determined. A 1-cm curvilinear grid was placed over the micrographs and membrane scored into the following categories: thin plasma membrane, dense membrane either with or without associated myofilaments. A membrane folding factor was calculated by normalizing to the subtended cross-sectional area for control and stretched muscle. These folding factors were then compared.

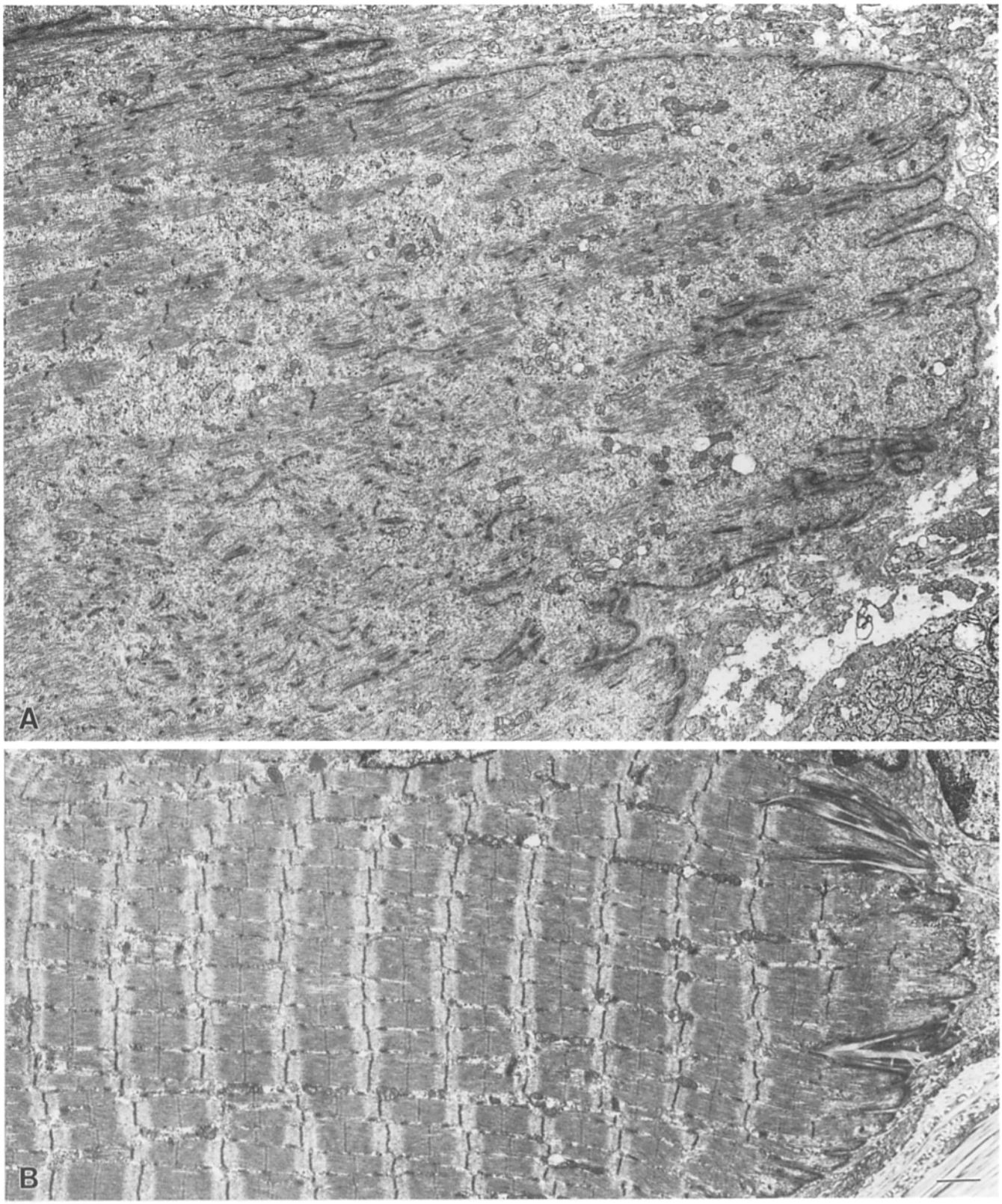

Figure 2. Ultrastructure at the MTJ of 4-d stretched and control fibers. (*A*) Stretched fiber MTJ with cytoplasmic space between myofibrils and the sarcolemma. This space is filled with developing myofibrils, polysomes, membrane systems, and mitochondria. (*B*) Control fiber MTJ with each myofibril attached to the sarcolemma at its final I-band. Bar, 1 μm.

Table I. Changes in the Sarcolemma at the Myotendinous Junction of Stretched Tibialis Anterior

	Control*	Stretched*
Membrane folding factor (S_{end}/cross section area)‡	1.0	0.74
Dense membrane		
With filaments (S_{Df}/S_{end})§	0.84	0.44
Without filaments (S_{Dwf}/S_{end})§	0.04	0.51
Nondense membrane (S_{ND}/S_{end})§	0.13	0.06

* Control values from six fibers from two muscles. Stretched values from 15 fibers from 4 4-d plantar-flexed muscles.
‡ Relative membrane surface areas determined using a 1-cm curvilinear grid (Eisenberg and Milton, 1984). Membrane folding factor gives membrane areas as a ratio of fiber area (S_{end}/cross section area). Folding factors expressed as a ratio of the control value.
§ Expressed as a fraction of total sarcolemmal area at fiber end (S_{end}).

Ultrastructural features at the myotendinous junction of fibers were cataloged by counting whether a particular feature was present or absent in each micrograph containing a known area of tissue after careful inspection of two independent observers.

Results

Myosin mRNA Accumulation

Casting the lower hindlimb of young adult rabbits in full plantarflexion resulted in rapid increases in TA weight and length expressed as a percent of the control legs. Weight increased 130.5 ± 7.6% at 4 d (n = 5 rabbits, mean ± SE) and 129.9 ± 3.5% at 6 d (n = 3 rabbits), and length increased 111.0 ± 1.7% at 4 d and 118.5 ± 0.5% at 6 d.

Muscle length increased by elongation of existing fibers. In situ hybridization revealed increased slow MHC mRNA at the MTJ of slow-oxidative fibers stretched for 4 d (Fig. 1 *A*) as compared to control fibers from the contralateral leg

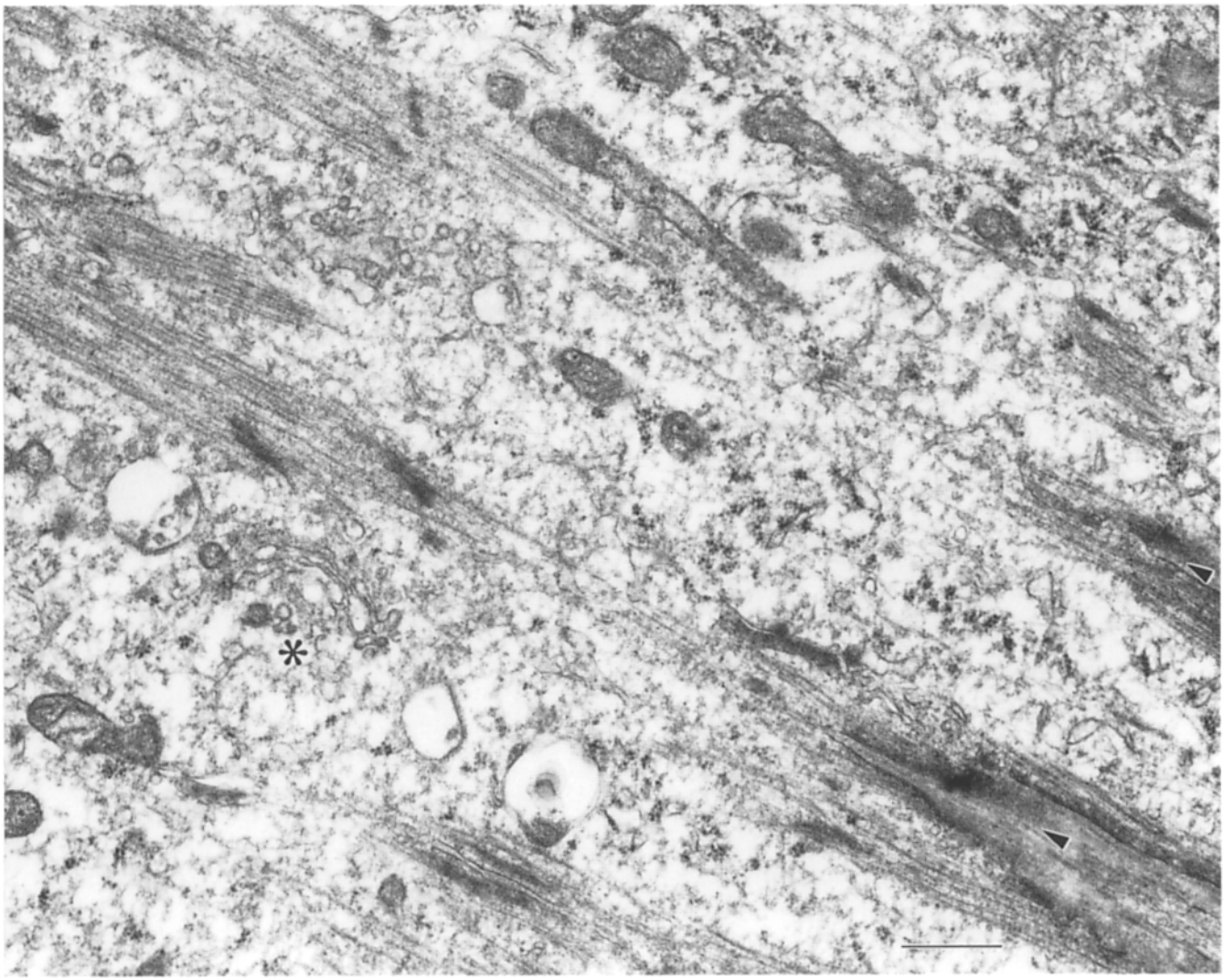

Figure 3. Myofibril attachment to sarcolemmal clefts at the MTJ of 4-d stretched fibers. Primarily thin filaments of elongating myofibrils cluster about membrane invaginations (*arrowheads*). Electron-dense material decorates the membrane at these attachment sites. This micrograph also includes a well-preserved Golgi stack (*asterisk*) and numerous polysomes between the myofibrils. Bar, 0.5 μm.

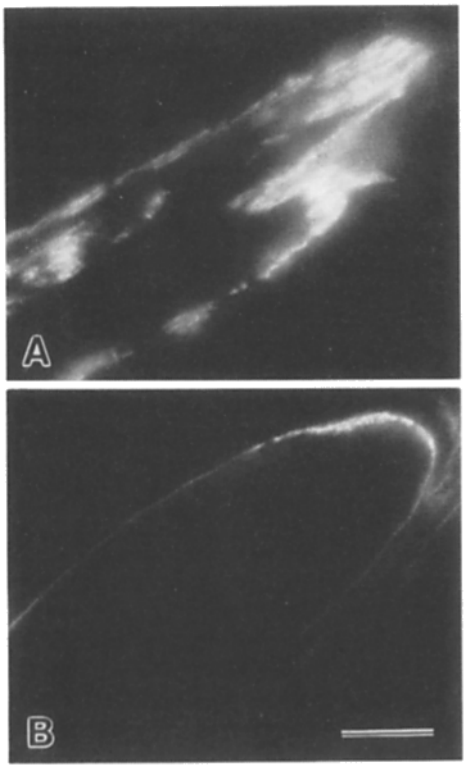

Figure 4. Immunofluorescent detection of vinculin at the MTJ of 4-d stretched and control fibers. (*A*) Stretched fiber with increased amount of vinculin on most of the sarcolemma at the MTJ. (*B*) Control fiber with limited area of MTJ with vinculin accumulation above background level found along sarcolemma throughout the fiber. Bar, 25 μm.

(Fig. 1 *B*). In the control fibers greater MHC mRNA concentrations are at the ends of fibers than in the midregion. This situation is exaggerated in the stretched muscles, which have an even greater concentration of MHC mRNA at their MTJ.

The area of the MTJ rich in MHC mRNA was expanded in the stretched fibers as compared to the control, and the subcellular distribution of MHC mRNA was not as organized. Longitudinal streaks of stain indicate intermyofibrillar concentrations, but at the tip of the fiber mRNA fills the cytoplasmic space without any pattern of distribution. Any further resolution of mRNA or polysome distributions required electron microscopy.

It was difficult to find slow-oxidative fibers at the distal end of control TA because most slow fibers terminated farther than 1 mm from the end of the last muscle fiber. There were even fewer slow fibers at the ends of stretch-hypertrophied muscles, where <5% of mature fibers express slow MHC.

Ultrastructural Changes

In stretched TA a large cytoplasmic space opened up between the myofibrils and the sarcolemmae of lengthening fibers (Fig. 2 *A*). Sarcolemmal invaginations or clefts were less developed in the stretched fibers, resulting in slightly reduced membrane folding factors for sarcolemmae at the MTJ (Table I). The MTJ of stretched fibers had a full complement of T-tubules and sarcoplasmic reticulum, and a greater amount of Golgi complexes and irregular sarcomeres (Fig. 3). Every MTJ of a stretched fiber observed had similar characteristics (15 fibers for 4 different animals). Control muscle fibers had no large cytoplasmic gaps between the thin filaments of the final sarcomere and the sarcolemma (Fig. 2 *B*).

Numerous polysomes were at the MTJ of stretched fibers. These polysomes were limited to intermyofibrillar sarcoplasm (Figs. 2 *A* and 3). Occasionally polysomes formed complexes at the end of forming thick filaments (data not shown), but this was more the exception than the rule. A microtrabecular lattice, observed in thin electron microscopy sections, was associated with the polysomes but we were not able to identify this lattice as any particular filament network.

Membranes and Attachment of Myofibrils at the Myotendinous Junction

Immunofluorescence with an antibody against vinculin faintly detected the sarcolemmae all along the fibers, but there was particular brightness at the MTJ. The intensity and range of membrane stained at the MTJ of stretched fibers (Fig. 4 *A*) was much greater than at the MTJ of control fibers (Fig. 4 *B*). The accumulations of vinculin at the MTJ of stretched fibers coincided with sarcolemmal densities throughout almost all of the MTJ membrane (Table I; Figs. 2 and 3).

A greater percentage of stretched fiber membranes had electron-dense accumulations (Fig. 2 and Table I). In control fibers, almost all membrane densities had contractile filaments attached to them. In stretched fibers this correspondence was lost; over half the membrane area with densities did not yet have filaments attached indicating that membrane changes precede myofibril formation.

Developing myofibrils attached to sarcolemmal clefts, though there was not always a continuum of thick and thin filaments connecting myofibrils to the cleft (Fig. 3). More often portions of the nascent myofibril thinned out to a few strands of thin or intermediate filaments. Sarcolemmal clefts were surrounded by a dense mesh of predominantly thin filaments oriented towards the extending myofibrils. The sarcolemmae contained electron-dense material at these attachment sites.

Myofibril Assembly

Many examples of myofibrillogenesis were found at the MTJ of stretched fibers as evidenced by a 20-fold increase in irregular sarcomeres. Careful analysis of these irregular sarcomeres suggests the various stages of assembly that comprise myofibrillogenesis at the MTJ. Electron micrographs of control fibers had only complete sarcomeres: aligned thin and thick filaments with straight, transverse Z-bands. Stretched fibers had many nonaligned thin and thick filaments. It was rare to see thin filament clusters without at least a few thick filaments, and only a very rare image of a solo thick filament was seen. There were also myofibrils with Z-bands added to the filaments, but the filaments were not always in sarcomeric register. Rarely were the thin and thick filaments in sarcomeric register without a readily identifiable Z-body present. Examination and counting many micrographs revealed that there were never Z-bodies in a myofibril without both thin and thick filaments. In other words, I-Z-I complexes were not seen.

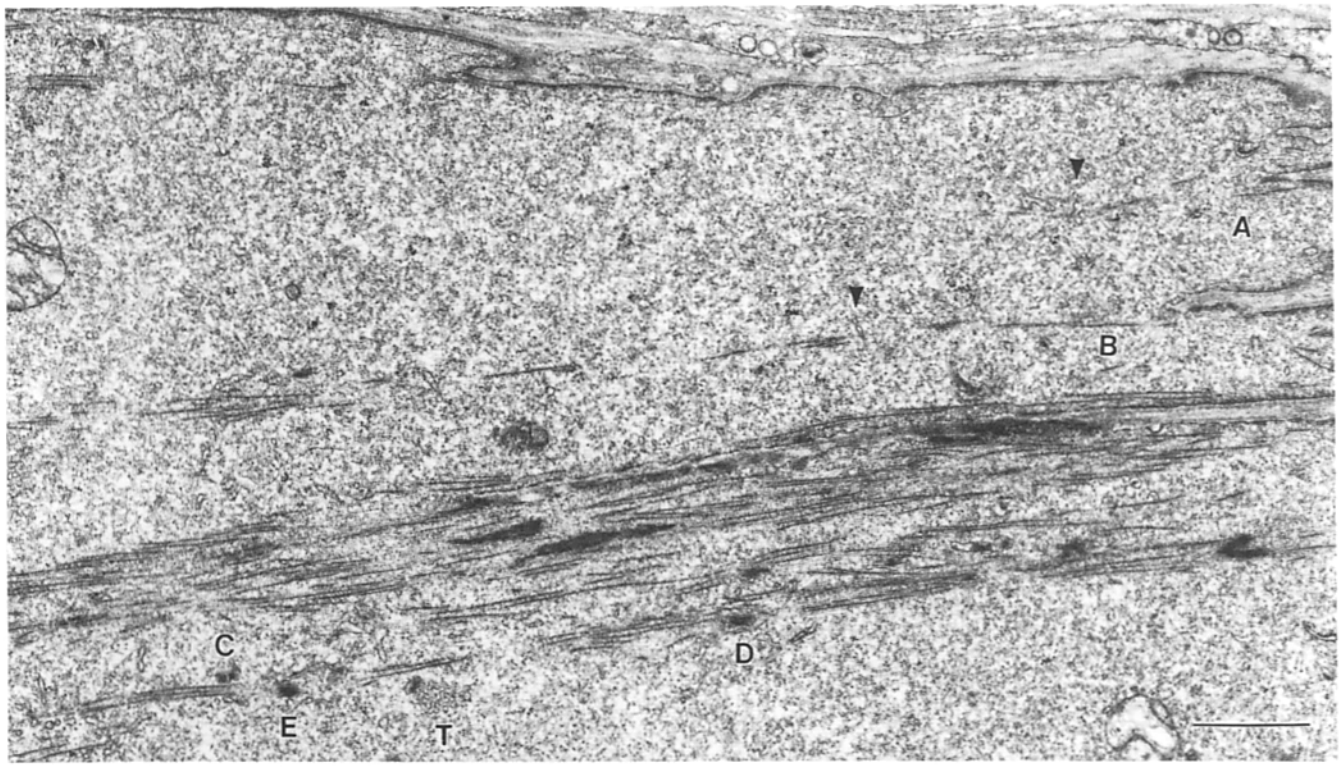

Figure 5. Myofibrillogenesis at the MTJ of a 4-d stretched fiber. Within this single fiber examples of the various stages of assembly are present (labeled *A–E*). (*A*) Clustering of a few thin filaments (and perhaps a few thicks) at a sarcolemmal cleft. (*B*) Thin and thick filaments directed longitudinally from a membrane cleft. Note the developing membrane triads within both of these nascent myofibrils (*arrowheads*, *A* and *B*). (*C*) Larger accumulation of thin and thick filaments without sarcomeric register. (*D*) Z-body attached to thin filaments, with thick filaments still not in sarcomeric register. (*E*) Z-body within an aligned segment of thin (I-band) and thick (A-band) filaments. Bar, 1 μm.

Quantitative tallies were made to record the order of appearance of the structural components of the myofibril. Examples of these different stages of assembly were all present within single fibers (Fig. 5). The quantitative results are presented as fractions in Table II and are used to interpret the most likely order of myofibrillogenesis.

Individual fibers sometimes exaggerated a particular aspect of myofibrillogenesis such as more Z-bands, more filaments, or more membranes. While all the stretched fibers had developing membrane systems amongst assembling myofibrils, several fibers had an unusually large number of T-tubule-like structures (Fig. 6) with disorganized filaments clustering around them. Other fibers exhibited many small Z-bodies which were closely spaced to one another (Fig. 2 *A*). These Z-bodies did not have an obvious pattern of distribution, linear or otherwise, within clusters of myofibrils.

Table II. Myofibril Characteristics at the Myotendinous Junction of Stretched Tibialis Anterior

	Control*	Stretched*‡
Thick filaments without Z-bodies		
No sarcomeric register	0	0.78
Sarcomeric register§	0	0.04
Thick filaments with Z-bodies		
No sarcomeric register	0	0.77
Sarcomeric register§	1.0	0.53
Z-bodies without thick filaments	0	0

* Control data from 20 micrographs of 6 fibers from 2 muscles. Stretched data from 60 micrographs of 15 fibers from 4 4-day plantarflexed muscles.
‡ Values presented are fractions of micrographs which exhibited at least one example of the structure listed. Some micrographs had more than one type of myofibril structure so sum is >1.0.
§ Sarcomeric register defined as alignment of thin and thick filaments into I-bands and A-bands respectively.

Myotube Formation

Transverse thick sections from the end of elongating 4-d muscles (within 1 mm of the last myofiber) contained few mature fibers expressing slow MHC (Fig. 7 *A*). However, for every four or five mature fibers a small myotube expressing slow MHC was present. After 6 d of stretch the majority of cells at the end of the muscle were myotubes (Fig. 7 *B*). Over 95% of these myotubes immunoreacted with the HPM-7 anti-slow MHC antibody. The myofibrils of these myotubes were not as tightly packed as in adult fibers, and the dark core in the fluorescent images of many of them was due to centrally located nuclei surrounded by a region devoid of fibrils.

The myotubes at the end of elongating fibers were filled with slow MHC mRNA. In situ hybridization of 6-d stretched muscle resulted in most of the myotubes stained throughout their core (Fig. 8 *A*). The mottled appearance was a result of light-staining nuclei and areas of the myotubes which were filling up with myofibrils. Control hybridizations

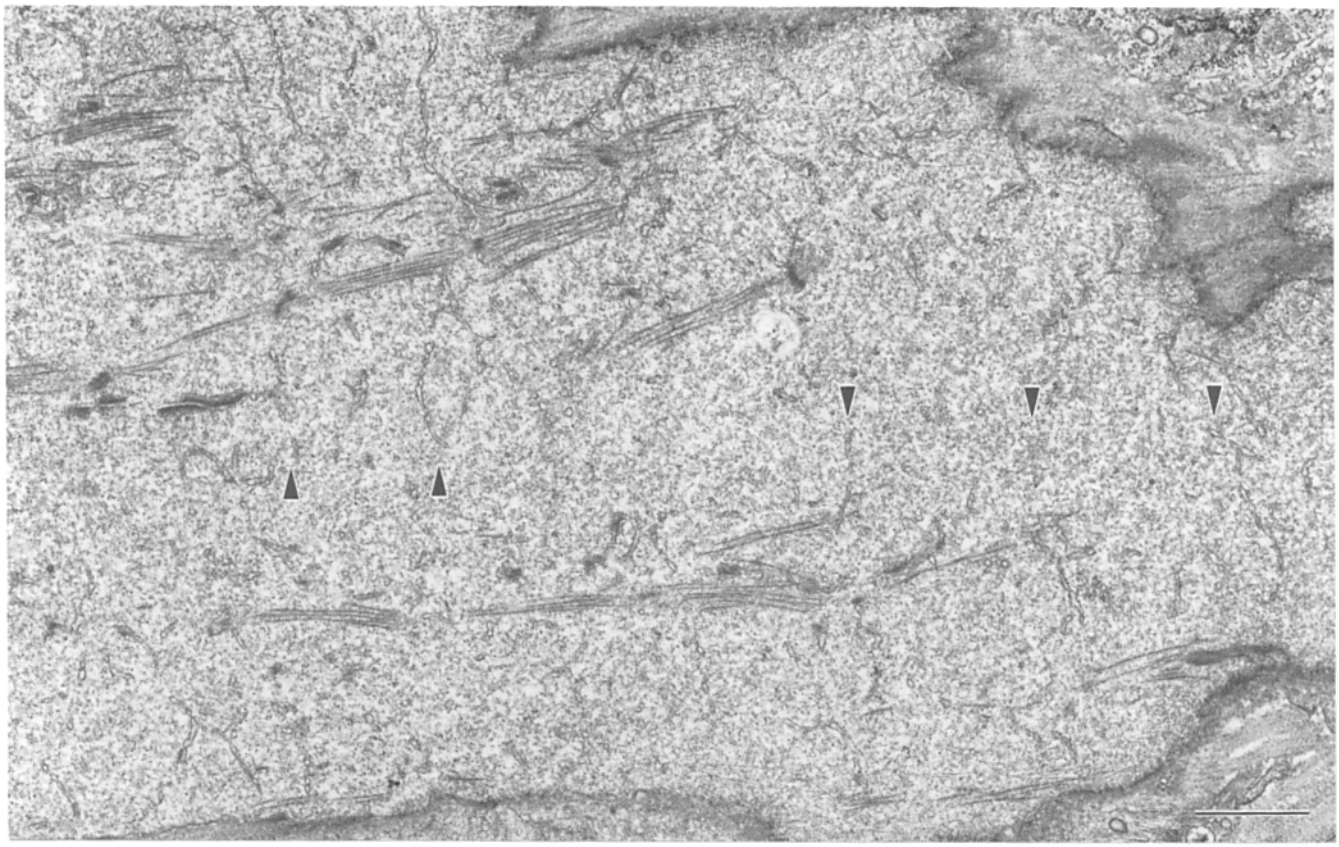

Figure 6. MTJ of a 4-d stretched fiber with a profusion of transverse membranes (*arrowheads*) in advance of myofibril development. Numerous thin and perhaps intermediate filaments are clustered under the sarcolemma and associated with these T-tubules. Myofibrils at various stages of assembly are interspersed as well. Bar, 1 μm.

with the sense-strand RNA probe resulted in very little background staining (Fig. 8 *B*).

Discussion

The accumulation of slow MHC mRNA at the MTJ of stretched slow-oxidative fibers was greater than in control fibers. Thus, a large number of MHC polysomes were located at the MTJ of elongating fibers, synthesizing MHC proximal to where it assembled into new sarcomeres. Possible mechanisms for directing MHC mRNA to the MTJ include the association of the mRNA with a specific structural element such as the cytoskeleton. MHC mRNA could accumulate where it is not spatially excluded by myofibrils. The increase in MHC mRNA could arise from myonuclei near the MTJ being programmed to transcribe a different set of genes from those elsewhere in the fiber or perhaps recently fused myoblast could be differentially transactivated. Not all these models require specific targeting mechanisms. Any of these hypotheses are compatible with our results at the MTJ of stretched fibers where MHC mRNA is concentrated in the large gap between the myofibrils and the sarcolemma. Similar concentrations of MHC mRNA were observed in regions of rapid growth and repair in the midregion of stretched fibers (Kennedy et al., 1988; Dix, D. J., and B. R. Eisenberg, unpublished observation).

The distance between the membrane and the bulk of the myofibrillar mass was greater in this chronic stretch model than in developmental (Tidball and Lin, 1989; Williams and Goldspink, 1971) and cultured cardiac cell models (Lin et al., 1989). The great distance spanned by the elongating myofibrils provided for expression of various stages of sarcomere assembly within individual fibers. Thin filaments attach to the talin-vinculin membrane complexes, anchoring the elongating myofibril and providing orientation to the assemblage.

Vinculin is a major component of myofibril attachment at the MTJ and is upregulated in response to stretch. Along with talin (Tidball et al., 1986) and α-actinin (Trotter et al., 1983), vinculin anchors the terminal thin filaments of the myofibrils. The membrane electron densities where myofibrils attached to the tendon are in part due to vinculin (Shear and Bloch, 1985). The increased vinculin densities throughout the sarcolemma at the MTJ make thin filament attachment possible at almost any location on the membrane.

Thin filaments first attach at the deeper clefts, or perhaps attachment causes the cleft to form at sites where all the essential molecular entities are first formed. Subsequent filament assembly tends to cluster about these primary locations. Thick filaments join thin filaments and at this point the T-tubules and sarcoplasmic reticulum membranes are often present. Z-bodies then assemble with the thin and thick filaments, coalesce into mature Z-bands, and set the filaments into sarcomeric register. The quantitative data from Table II

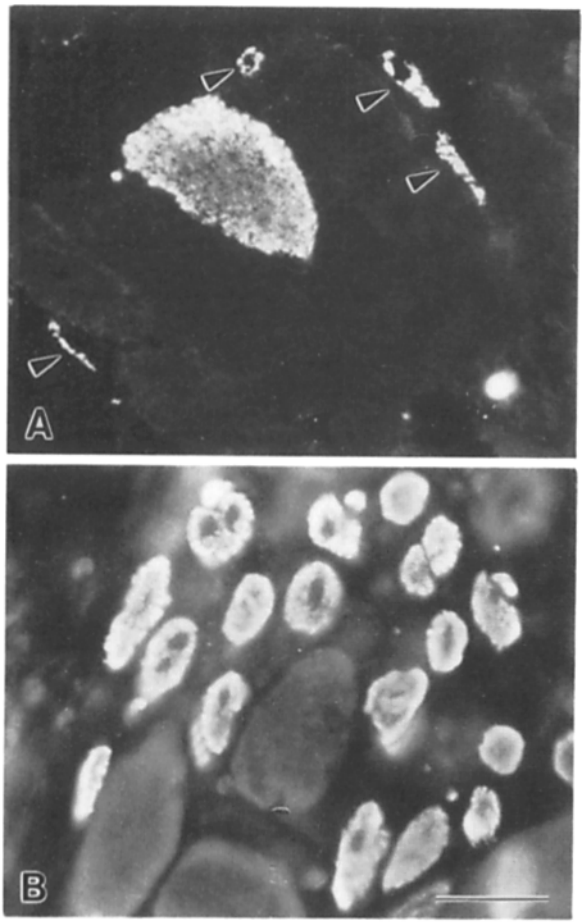

Figure 7. Myotubes at the ends of TA after 4- and 6-d stretch. (*A*) Immunofluorescent detection of slow MHC identifies four small myotubes (*arrowheads*) and one preexisting slow-oxidative fiber at the end of TA stretched for 4-d. (*B*) Many slow MHC-expressing myotubes are present after 6-d stretch, accounting for the majority of cells at the end of the lengthening muscle. Bar, 50 μm.

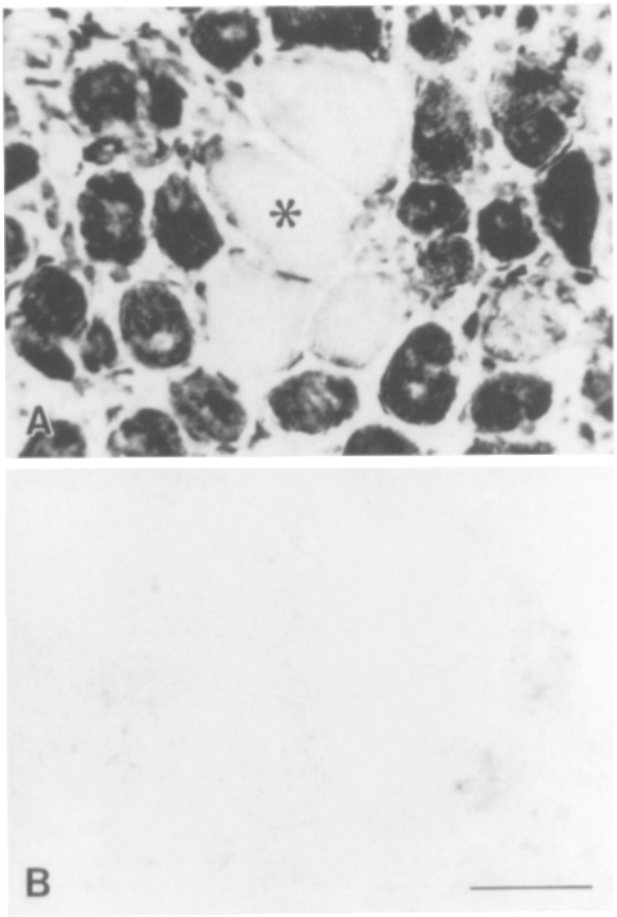

Figure 8. In situ hybridization of MHC mRNA in myotubes at the ends of TA stretched for 6 d. (*A*) ISH with an anti-sense RNA probe demonstrates the dense nonspecific distribution of slow MHC mRNA in myotubes. Four larger fibers in center of field are preexisting fast fibers (*asterisk*). (*B*) Negative control ISH with the sense RNA probe resulted in low background staining. Bar, 50 μm.

is used to construct a graphic representation of this process in a single myofibril (Fig. 9).

By comparing our observations with existing theories on myofibril assembly, the following can be stated. We very rarely saw thick filaments not associated with thin filaments. It seems likely that myosin assembles into thick filaments on an actin filament template as suggested by fluorescence energy transfer studies in *Dictyostelium* (Mahajan et al., 1989). Stress fiber–like structures acting as templates for developing myofibrils (Dlugosz et al., 1984) were not seen in any stretched or control fibers. At the earliest stages of myofibril assembly when only a few thin filaments and perhaps intermediate filaments were observed, we saw thick filaments adding directly to these sparse structures in an unregistered manner. Small aggregates of α-actinin, which coalesce into mature Z-bands (McKenna et al., 1986), are more in agreement with our observations than the idea of minisarcomeres (Sanger et al., 1986). The postulate that Z-bodies (and associated titin filaments) are required for setting sarcomeric register (Hill et al., 1986; Lin et al., 1989; Tokuyasu and Maher, 1987*a*, *b*) seems reasonable since we saw few aligned filaments in myofibrils without Z-bodies. Z-bodies seem to be required to determine polarity of the thin filaments and allow registration of the thick filaments into A-bands. However, Z-bodies or I-Z-I complexes are not a requirement for thin and thick filament assembly (Beall et al., 1989).

Some heterogeneity should be recognized in fiber strategies for growth. Fibers with exaggerated features such as profligate T-tubules (Fig. 6) or Z-bodies which form a striped pattern (Fig. 1 *A*) can be taken as extreme examples of various components of myofibrillogenesis. These could also be examples of uncoordinated gene expression in response to stretch. Regional overexpression of a particular muscle protein could be a result of unbalanced nuclear domains. Stretch-activated nuclei may also be more susceptible to overexpression of a single gene product.

Nascent fibers and myotubes at the ends of muscles stretched for 6 d are another example of stretch activation. It is expected that these myotubes will fuse with and become extensions of existing fibers, similar to what is observed during development (Moss and Leblond, 1971; Williams and Goldspink, 1971). Essentially all of the myotubes expressed slow MHC. This is a recapitulation of the developmental

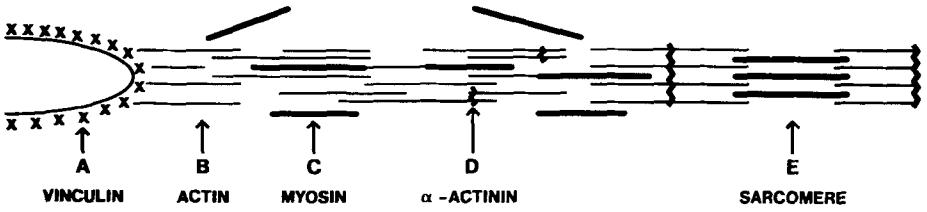

Figure 9. Myofibrillogenesis at the MTJ of stretched skeletal muscle. Vinculin (*A*) corresponds to the sarcolemmal electron densities which anchor actin thin filaments (*B*). Myosin thick filaments (*C*) aggregate with the thin filaments, and α-actinin Z-bodies (*D*) then align these filaments into sarcomeric register (*E*).

program of isomyosin expression. All primary myotubes in the developing rat TA express slow MHC as well (Narusawa et al., 1987) and a reversion to the embryonic phenotype was observed in stretched chicken muscle (Kennedy et al., 1988, 1989). The RNA probe and antibody used to detect slow MHC expression have proven their specificity in numerous applications (Dix and Eisenberg, 1988; Kennedy et al., 1986).

The intracellular distribution of MHC mRNA in myotubes is less organized than seen in adult fibers. A more homogenous distribution of MHC mRNA was also reported in cultured myotubes (Singer et al., 1987) and in developing rabbit fibers (Dix, D. J., and B. R. Eisenberg, unpublished data). It seems the organization of the myofibrils plays a large role in determining MHC mRNA distribution because mRNA is excluded from the orderly myofilament lattice.

In conclusion, we found that a large cytoplasmic space devoid of myofibrils forms at the ends of stretched fibers and fills with MHC mRNA. These local accumulations of mRNA provide for regional synthesis of contractile proteins, rapid sarcomere assembly, and extension of the myofibrils. Myofibrillogenesis proceeds first by preparing the membrane for attachment, then thin and thick filament aggregation. Sarcomeric register is set by Z-bodies which add into the filament bundles. The stretched muscles also lengthen by the proliferation of myotubes at the MTJ.

The authors would like to thank Ms. P. Larramendi for excellent technical assistance.

The work was supported by National Institutes of Health grant HL 40880 and Muscular Dystrophy Association. D. J. Dix was supported in part by National Research Service Award T32 HL 07320.

Received for publication on April 1990 and in revised from 10 July 1990.

References

Antin, P. B., S. Tokunaka, V. T. Nachmias, and H. Holtzer. 1986. Role of stress fiber-like structures in assembling nascent myofibrils in myosheets recovering from exposure to ethyl methanesulfonate. *J. Cell Biol.* 102:1464–1479.

Beall, C. J., M. A. Sepanski, and E. A. Fyreberg. 1989. Genetic dissection of Drosophila myofibril formation: effects of actin and myosin myosin heavy chain null alleles. *Gene & Dev.* 3:131–140.

Bouche, M., S. M. Goldfine, and D. A. Fischman. 1988. Posttranslational incorporation of contractile proteins into myofibrils in a cell-free system. *J. Cell Biol.* 107:587–596.

Dix, D. J., and B. R. Eisenberg. 1988. In situ hybridization and immunocytochemistry in serial sections of rabbit skeletal muscle to detect myosin expression. *J. Histochem. Cytochem.* 6:1519–1526.

Dlugosz, A. A., P. B. Antin, V. T. Nachmias, and H. Holtzer. 1984. The relationship between stress fiber-like structures and nascent myofibrils in cultured cardiac myocytes. *J. Cell Biol.* 99:2268–2278.

Eisenberg, B. R., J. M. Kennedy, M. P. Wenderoth, and D. J. Dix. 1989. Satellite cells, isomyosin switching and muscle growth. *In* Cellular and Molecular Biology of Muscle Development. L. Kedes and F. Stockdale, editors. Alan R. Liss, Inc., New York., 451–460.

Eisenberg, B. R., and R. L. Milton. 1984. Muscle fiber termination at the tendon in the frog's sartorius: a stereological study. *Am. J. Anat.* 171:273–284.

Fontaine, B., D. Sasson, M. Buckingham, and J. Changeux. 1988. Detection of the nicotinic acetylcholine receptor α-subunit mRNA by in situ hybridization at neuromuscular junctions of 15-day-old chick striated muscles. *EMBO (Eur. Mol. Biol. Organ.) J.* 7:603–609.

Goldspink, G. 1985. Malleability of the motor system: a comparative approach. *J. Exp. Biol.* 115:375–391.

Hill, C. S., S. Duran, Z. Lin, K. Weber, and H. Holtzer. 1986. Titin and myosin, but not desmin, are linked during myofibrillogenesis in postmitotic mononucleated myoblasts. *J. Cell Biol.* 103:2185–2196.

Johnson, C. S., N. M. McKenna, and Y. Wang. 1988. Association of microinjected myosin and its subfragments with myofibrils in living muscle cells. *J. Cell Biol.* 107:2213–2221.

Kennedy, J. M., S. Kamel, W. W. Tambone, G. Vrbova, and R. Zak. 1986. The expression of myosin heavy chain isoforms in normal and hypertrophied chicken slow muscle. *J. Cell Biol.* 103:977–983.

Kennedy, J. M., B. R. Eisenberg, S. K. Reid, L. J. Sweeney, and R. Zak. 1988. Nascent muscle fiber appearance in overloaded chicken slow-tonic muscle. *Am. J. Anat.* 181:203–215.

Kennedy, J. M., L. J. Sweeney, and J. Gao. 1989. Ventricular myosin expression in developing and regenerating muscle, cultured myotubes, and nascent myofibers of overloaded muscle in chicken. *Med. Sci. Sports Exercise.* 21:S187–197.

Lawrence, J. B., and R. H. Singer. 1986. Intracellular localization of messenger RNAs for cytoskeletal proteins. *Cell.* 45:407–415.

Lin, Z., S. Holtzer, T. Schultheiss, J. Murray, T. Masaki, D. A. Fischman, and H. Holtzer. 1989. Polygons and adhesion plaques and the disassembly and assembly of myofibrils in cardiac myocytes. *J. Cell Biol.* 108:2355–2367.

Mahajan, R. K., K. T. Vaughan, J. A. Johns, and J. D. Pardee. 1989. Actin filaments mediate Dictyostelium myosin assembly in vitro. *Proc. Natl. Acad. Sci. USA.* 86:6161–6165.

McKenna, N., C. Johnson, and Y. Wang. 1986. Formation and alignment of Z lines in living chick myotubes microinjected with rhodamine-labeled alpha-actinin. *J. Cell Biol.* 103:2163–2171.

Merlie, J. P., and J. R. Sanes. 1985. Concentration of acetylcholine receptor mRNA in synaptic regions of adult muscle fibres. *Nature (Lond.).* 317:66–68.

Moss, F. P., and C. P. Leblond, 1971. Satellite cells as the source of nuclei in muscles of growing rats. *Anat. Rec.* 70:421–436.

Narusawa, M., R. B. Fitzsimons, S. Izumo, B. Nadal-Ginard, N. A. Rubinstein, and A. M. Kelly. 1987. Slow myosin in developing rat skeletal muscle. *J. Cell Biol.* 104:447–459.

O'Donnell, P. T., and S. I. Bernstein. 1988. Molecular and ultrastructural defects in a *Drosophila* myosin heavy chain mutant: differential affects on muscle function produced by similar thick filament abnormalities. *J. Cell. Biol.* 107:2601–2612.

Saad, A. D., J. D. Pardee, and D. A. Fischman. 1986. Dynamic exchange of myosin molecules between thick filaments. *Proc. Natl. Acad. Sci. USA.* 83:9483–9487.

Sanger, J. M., B. Mittal, M. B. Pochapin, and J. W. Sanger. 1986. Myofibrillogenesis in living cells microinjected with fluorescently labeled alpha-actinin. *J. Cell Biol.* 102:2053–2066.

Schmidt, V. 1927. Die histogenese der quergestreiften muskelfaser und des muskelsehnenuberganges. *Z. Mikrosk. Anat. Forsch. (Leipz.).* 8:97–184.

Shear, C. R., and R. J. Bloch. 1985. Vinculin in subsarcolemmal densities in chicken skeletal muscle: localization and relationship to intracellular and extracellular structures. *J. Cell Biol.* 101:240–256.

Singer, R. H., J. B. Lawrence, G. L. Langevin, R. N. Rashtchian, C. A. Villnave, T. Cremer, D. Tesin, L. Manuelidis, and D. C. Ward. 1987. Double labeling in situ hybridization using non-isotopic and isotopic detection. *Acta Histochem. Cytochem.* 20:589–599.

Sinha, A. M., D. J. Friedman, J. M. Nigro, S. Jakovcic, M. Rabinowitz, and P. K. Umeda. 1984. Expression of rabbit ventricular alpha-myosin heavy chain messenger RNA sequences in atrial muscle. *J. Biol. Chem.* 259: 6674–6680.

Tidball, J. G., and C. Lin. 1989. Structural changes at the myogenic cell surface during the formation of myotendinous junctions. *Cell Tissue Res.* 257:77–84.

Tidball, J. G. T. O'Halloran, and K. Burridge. 1986. Talin at myotendinous junctions. *J. Cell Biol.* 103:1465–1472.

Tokuyasu, K. T., and P. A. Maher. 1987*a*. Immunocytochemical studies of cardiac myofibrillogenesis in early chick embryos. I. Presence of immunofluorescent titin spots in premyofibril stages. *J. Cell Biol.* 105:2781–2793.

Tokuyasu, K. T., and P. A. Maher. 1987*b*. Immunocytochemical studies of cardiac myofibrillogenesis in early chick embryos. II. Generation of alpha-actinin dots within titin spots at the time of the first myofibril formation. *J. Cell Biol.* 105:2795–2801.

Trotter, J. A., S. Eberhard, and A. Samora. 1983. Structural domains of the muscle-tendon junction. 1. The internal lamina and the connecting domain. *Anat. Rec.* 207:573–591.

Wenderoth, M. P., and B. R. Eisenberg. 1987. Incorporation of nascent myosin heavy chains into thick filaments of cardiac myocytes in thyroid-treated rabbits. *J. Cell Biol.* 105:2771–2780.

Williams, P. E., and G. Goldspink. 1971. Longitudinal growth of striated muscle fibers. *J. Cell Sci.* 9:751–767.

Williams, P. E., and G. Goldspink. 1973. The effect of immobilization on the longitudinal growth of striated muscle fibers. *J. Anat.* 116:45–55.